



## Head and Neck Squamous Cell Carcinoma: Cuproptosis-related Long Non-coding RNAs Predict Prognosis and Immunotherapeutic Response

Tao Liang<sup>1</sup>, Yuanzhi Zhu<sup>1</sup>, Yi Huang<sup>1</sup>, Yao Ding<sup>1</sup>, Shizi Wang<sup>1</sup>, Xiaoqiang Mo<sup>1\*</sup>

<sup>1</sup> Youjiang Medical University for Nationalities, No. 98 Countryside Road, BaiseGuangxi 533000, China

\* Corresponding author: Xiaoqiang Mo E-mail: 29109799@qq.com

**Abstract: Objective** Head and neck squamous cell carcinoma (HNSCC) has a poor prognosis because of high recurrence and metastasis rates and failure of immunotherapy caused by escape of immune cells. The aim of this study was to explore potential biomarkers and precise drug therapies for HNSCC.

**Methods** We extracted the RNA transcriptome dataset and related clinical data of patients with HNSCC from The Cancer Genome Atlas (TCGA) database to analyze differentially expressed long non-coding RNAs (lncRNAs) in HNSCC. We screened differentially expressed lncRNAs related to cuproptosis among regulatory genes and identified those that best indicated the prognosis of HNSCC univariate Cox (uni-Cox) regression analyses and the least absolute shrinkage and selection operator. We constructed models and evaluated their accuracy in determining high- and low-risk groups using the Kaplan–Meier, receiver operating characteristic curve, and uni-Cox regression and multivariate Cox (multi-Cox) regression analyses. Subsequently, we subjected the high-risk group to gene set variation analysis, principal component analysis, immunoassay, and half-maximal inhibitory concentration prediction. To further improve tumor immunotherapy, we divided the entire sample into cold and hot groups based on cuproptosis-related lncRNAs and analyzed the therapeutic differences. **Results** Combined with cuproptosis-related genes and by analyzing the HNSCC data from TCGA, we obtained five cuproptosis-related prognostic lncRNAs. The model showed certain reliability. Patients in the high- and low-risk groups had different tumor microenvironments and drug sensitivities. Cuproptosis-related lncRNA expression differed between cold and hot tumors. Further, hot tumors were more sensitive to immunotherapy drugs compared to cold tumors.

**Conclusion** This study established and verified the lncRNAs that stratified the prognostic risk related to cuproptosis in HNSCC. The model also predicted immunotherapeutic responses of patients with HNSCC and provided a reference for the individualized treatment of cold and hot tumors.

**Keywords** Cuproptosis ; lncRNA ; HNSCC; Immunotherapy ; TCGA

### 1. Introduction

Among humans, disease is the leading cause of death, with cancer being the second most common. Head and neck cancers is one of the eight most common cancers reported worldwide. In the past decade, the incidence of head and neck squamous cell carcinoma (HNSCC), the main pathological type of head and neck cancer, has increased significantly. The treatment of HNSCC is surgical resection and postoperative radiotherapy; however, its high metastasis and recurrence rates lead to a low survival rate. Therefore, novel treatment strategies to improve patient survival should be explored. Immunotherapy is an emerging treatment for cancer. Many patients with HNSCC have innate and adaptive immune deficiencies, including dendritic and T-cell dysfunction. Current treatment modalities, including surgery, radiotherapy, and chemotherapy, may exacerbate this cellular immune deficiency. Compared to other treatment methods, immunotherapy can better improve patients' quality of life. Moreover, HNSCC is a high immune-infiltrating tumor; therefore, immunotherapy could yield a better therapeutic effect <sup>1</sup>.

As an essential trace element in the human body, copper is maintained at a certain concentration under normal physiologic conditions and plays an important role in many biochemical reactions, including redox processes and hemoglobin synthesis. However, copper is an environmental pollutant. With industrial development, industrial mining and smelting, metal processing, machinery manufacturing, steel production, etc., have significantly polluted the environment. Moreover, copper pollution in rivers has been reported worldwide. Excessive copper entering the human body can disturb its metabolism and damage heart, liver, and kidney functions <sup>2</sup>. Elevated copper has also been found in cancer tissues. The relationship between copper and tumorigenesis remains controversial. Elevated copper has been found to influence the formation and growth of malignancies. Significant changes in copper levels have been found in cancer tissue and serum of patients with cancer, including oral, lung, thyroid, and gastric cancers <sup>3</sup>. In contrast, high copper concentrations have also been found to cause the death of cancer cells. The underlying mechanism is called cuproptosis. Cuproptosis in cells mainly involves 10 genes: *FXD1*, *LIAS*, *LIPT1*, *DLG*, *DLAT*, *PDHA1*, *PDHB*, *MTF1*, *GLS*, and *CDKN2A*.

In recent years, long non-coding RNA (lncRNA), as a kind of non-coding RNA with a length of more than 200 nucleotides, has been gradually recognized to have a broad application prospect in oncology with the in-depth study of its structure,



distribution, and physiological function. It has become a rigorously studied topic in molecular biology. Aberrantly expressed lncRNAs have been detected in various types of cancers, some exhibiting oncogenic or tumor-suppressive effects, suggesting their potential as biomarkers and therapeutic targets of tumors<sup>4,5</sup>. Furthermore, lncRNA influences cancer cell proliferation, apoptosis, invasion, and metastasis. In HNSCC, it can also affect tumor occurrence and development by regulating tumor-promoting or tumor-suppressor genes. In addition, it can regulate gene expression and affect cancer prognosis and chemotherapy resistance<sup>6</sup>. It can also promote tumor inflammation and help tumors escape immune destruction<sup>7</sup>. Immunotherapy, an emerging treatment for HNSCC, involves immune checkpoint inhibitors. Existing immunotherapies have limitations, such as the toxicity of immunotherapy drugs and the lack of immunotherapeutic responses. Tumors that do not respond to immunotherapy are called “cold” tumors. Their center and margin areas are almost devoid of immune cells. In contrast, “hot” tumors have a high density of immune cells and are sensitive to immune checkpoint inhibitors<sup>8</sup>. To date, there has been no study on cuproptosis-related lncRNAs as potential therapeutic targets for HNSCC. Therefore, gaining more knowledge of cuproptosis-related lncRNAs can not only help us to understand more clearly the roles of cuproptosis and lncRNAs in immunotherapy, but also help us to reconstitute patients according to cuproptosis-related lncRNAs to differentiate between cold and hot tumors, and further explore differences in immunotherapies that can be precisely regulated during treatment.

## 2. Materials and Methods

### 2.1 Data sources

RNA sequencing and clinical data of patients with HNSCC were downloaded from The Cancer Genome Atlas (TCGA) website (<http://www.tcg.org>). We extracted 502 HNSCC and 44 normal tissue samples. Clinical data comprised sex, age, tumor grade, tumor pathological stage, TNM stage, survival time, and survival status. All tumor samples were of solid tumors.

### 2.2 Screening of cuproptosis-related lncRNAs

The differential expression analysis was performed on HNSCC data downloaded from TCGA database using Strawberry Perl and “limma” R package. Criteria for statistical significance were: false discovery rate < 0.05;  $|\log_2$  fold change| > 1; and  $p < 0.05$ . Subsequently, based on the 10 cuproptosis-related genes reported in literature, the expression correlation analysis was performed, and lncRNAs related to cuproptosis gene expression were screened.

### 2.3 Model construction and validation

In TCGA database, patients with a follow-up duration < 30 days and missing overall survival (OS) were excluded. The overall cohort was divided into training and test groups at random. The model is constructed by training group and the predictive ability of the model is verified by testing group. The screen differentially expressed cuproptosis-related lncRNAs were analyzed for their sensitivity to predict the prognosis. The lncRNAs related to the prognosis were screened using univariate Cox (uni-Cox) regression. For model construction, to reduce accidental errors caused by a single division of the training and test groups, we performed a ten-fold cross-validation using least absolute shrinkage and selection operator (LASSO) regression. In the regression analysis, to prevent overfitting, which often occurs because of the poor performance of the validation dataset and causes bias, we ran 1,000 cycles to reduce contingency, and created a predictive model for cuproptosis-related lncRNAs. After successful construction, the model’s sensitivity and specificity were verified using “survivalROC” package of R software combined with the receiver operating characteristic (ROC) curves of 1, 2, and 3 years. The area under the ROC curve (AUC) was calculated to evaluate the effectiveness of the model. AUCs of < 0.5, 0.51–0.70, 0.71–0.9, and > 0.9 indicated no predictive ability, low accuracy, medium accuracy, and high accuracy, respectively. Calibration curves were drawn to determine the prediction accuracy.

We choose the following formula to calculate the risk score (RS) :

$$RS = \sum_{i=1}^n \text{Coef}(i) \times x(i)$$

Coef( $i$ ) represents the regression coefficient obtained using multivariate Cox (multi-Cox) regression, and  $x(i)$  represents the expression data of each lncRNA. Patients were divided into high- and low-risk groups according to the median risk score. Independent prognostic factors were screened using the chi-square test and uni-Cox and multi-Cox regression. Whether or not the risk score in the model was an independent prognostic factor for patients with HNSCC was verified.

### 2.4 Nomogram construction and verification

After screening the independent prognostic factors of HNSCC, including age, tumor stage, and risk score, nomograms of 1-, 2-, and 3-year survival rates were constructed. Since the conclusion of this study depended strongly on the constructed model’s ability to make predictions, the Hosmer–Lemeshow test was used to verify whether or not our hypothesized model met the requirements before obtaining the results.

### 2.5 Gene set variation analysis (GSVA)

GSVA is a non-parametric test used to calculate the genome-specific enrichment score of each sample, reflecting the connections between samples and signaling pathways. It is a computational method to study microarray data at the gene set level. To predict changes in pathway activity and biological functions of the signaling pathways involved in the high- and low-risk groups, GSVA was utilized to examine the relationship between the two groups. Criteria for statistical significance were: false discovery rate < 0.25 and  $p < 0.05$ .

### 2.6 Immune checkpoints and tumor microenvironment (TME)

Abnormal changes in TME not only affect the prognosis of patients, but also can be used as a biomarker for immunotherapy. After the GSVA results were obtained, tumor immune cell infiltration data from different platforms, such as xCell, Timer, and quanTIseq, were used to investigate the association between TME immune cell infiltration and the high-risk group. The

“ggplot2” package was used to draw bubble plots.

### 2.7 Genomics of drug sensitivity in cancer (GDSC) analysis

To explore the use of models in clinical treatment, the GDSC database was developed by the Sanger Institute in the United Kingdom. It contains the sensitivity data and the corresponding genomic data of different drugs in tumor cell lines. Therefore, it has a great significance in the development of medicine. It can be used to discover potential tumor therapeutic targets or assess whether or not the target has more sensitive therapeutic drugs. The half-maximal inhibitory concentration (IC50), a frequently used parameter in drug research, is often used as an index to explore resistance and sensitivity of cancer drugs. It can also be used to assess drugs’ capacity to trigger apoptosis, with lower values indicating stronger inducing abilities. In addition, it can be used to study drug resistance of cells, indicating the degree of tolerance simultaneously. We calculated IC50 using the “pRRophetic” R package to explore the model’s clinical application value.

### 2.8 Differentiation of hot and cold tumors and exploration of their roles

To explore differences in patients with HNSCC according to the immunotherapeutic response, we divided them into subgroups by cuproptosis-related lncRNAs. With continuously increasing data generation and collection, visualizing and drawing inference maps become increasingly difficult. For dimensionality reduction of data, we used the principal component analysis (PCA) and t-distributed stochastic neighbor embedding. To verify the differences between them after identifying the subpopulations in HNSCC, we used the Kaplan–Meier analysis for survival comparison. In addition, we compared TME and drug sensitivity between the two groups.

## 3. Results

### 3.1 Cuproptosis-related genes in patients with HNSCC

Figure 1A shows the results of the screening of the differentially expressed lncRNAs between patients with HNSCC and healthy controls from TCGA database. Figure 1B shows the results of the screening of the cuproptosis-related lncRNAs based on the 10 cuproptosis-related genes. Figure 1C shows the interaction network between the cuproptosis-related genes and lncRNAs.

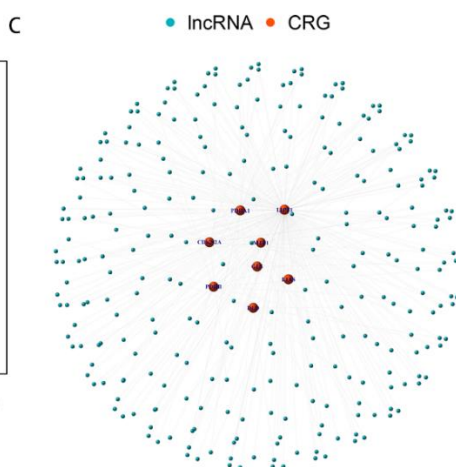
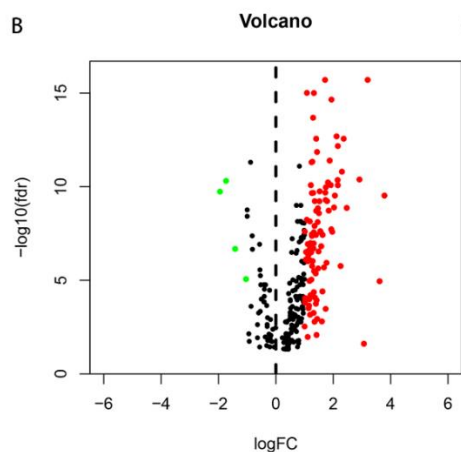
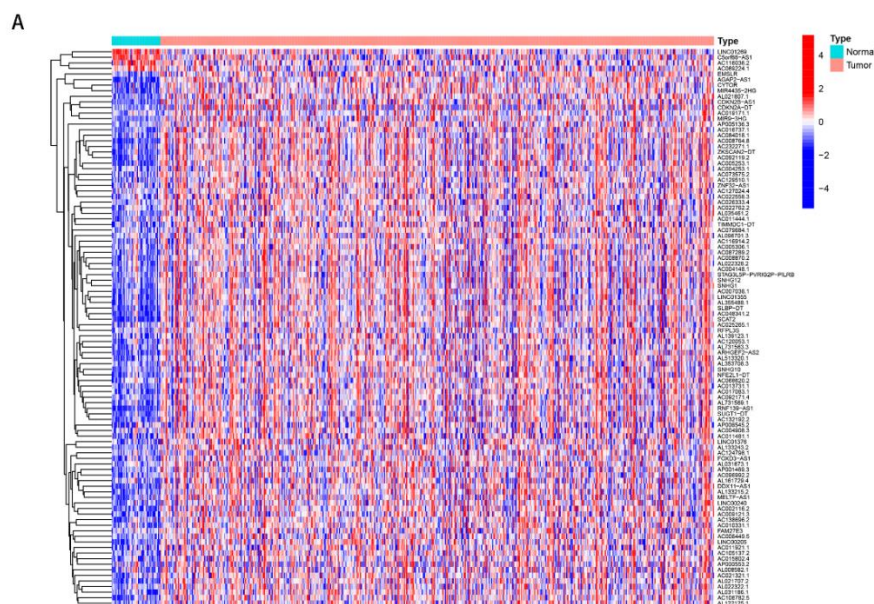


Figure 1. Expression and identification of cuproptosis-related lncRNAs in patients with HNSCC. (A) Gene heat map of differentially expressed cuproptosis-related lncRNAs. (B) Volcanic map of differentially expressed cuproptosis-related lncRNAs. (C) Network diagram between cuproptosis genes and lncRNAs.

### 3.2 Model construction and certification

uni-Cox regression showed that 16 cuproptosis-related lncRNAs were associated with OS (Figure 2A,  $p < .05$ ). Figure 2B shows the heat map. LASSO regression analysis was used to reduce the deviation of the data (Figure 2C and 2D). In HNSCC, 15 lncRNAs associated with copper death were up-regulated, whereas one lncRNA was down-regulated (Figure 2E). The analysis and formula showed five copper death-related lncRNAs in HNSCC. Using the RS formula, we re-ranked the training and test groups and the overall cohort according to the RS obtained by each sample and plotted risk curves of the RS and the survival status. The abscissa of the curve was the order of patients, ascending from left to right by RS. The SR was the vertical axis of the curve. Figure 3A shows the plotting of the RS value on the risk curve and dividing patients into high- and low-risk groups based on the median value. The results of the relationship between survival time in high- and low-risk groups are presented in the scatter plot: Blue represents survival, and red represents death. Red dots increase from left to right. In the low-risk area, blue dots are clustered, whereas in the high-risk area, red dots are clustered (Figure 3B). Expressions of five cuproptosis-related lncRNAs in the high- and low-risk groups were also plotted, among which *FAM27E3* and *MIR4435-2Hg* were overexpressed in the high-risk group, while *FAM27E3*, *AC021321.1*, and *AL513320.1* were underexpressed (Figure 3C). The Kaplan-meier analysis also showed that the survival prognosis of HNSCC patients was significantly different between the high and low risk groups, and the high risk group had a worse prognosis (Figure 3D,  $p < .05$ ). Figure 3E shows the relationship between RS and tumor stage characteristics (Figure 3E). The above results fully indicate that the high-risk group of HNSCC patients has a worse prognosis and a higher mortality rate.

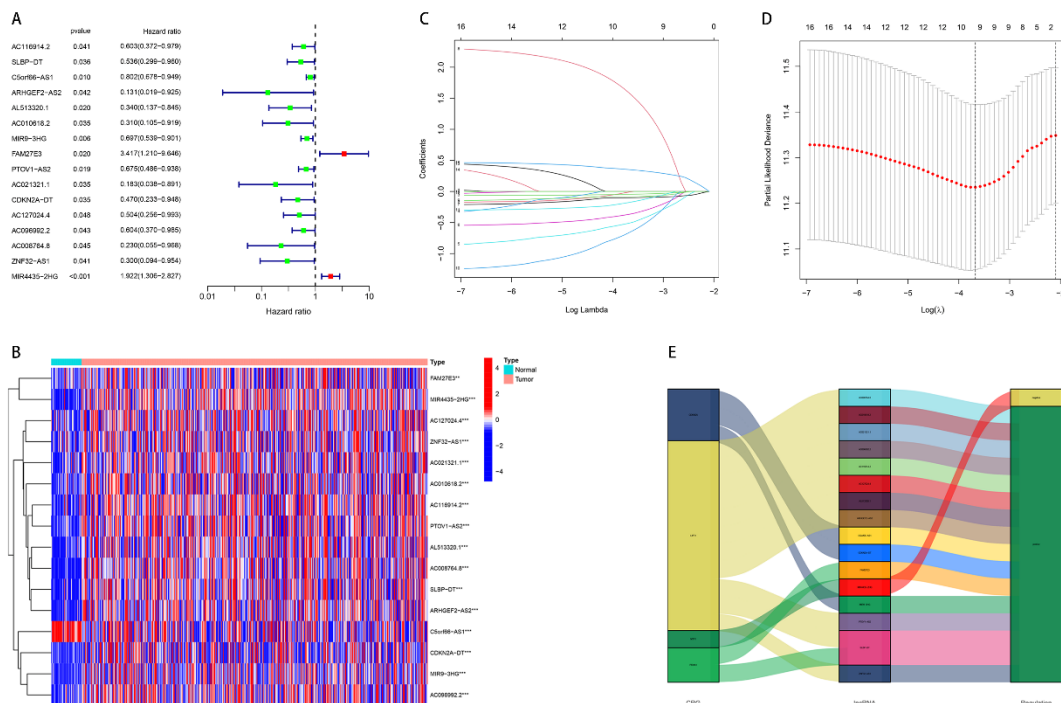
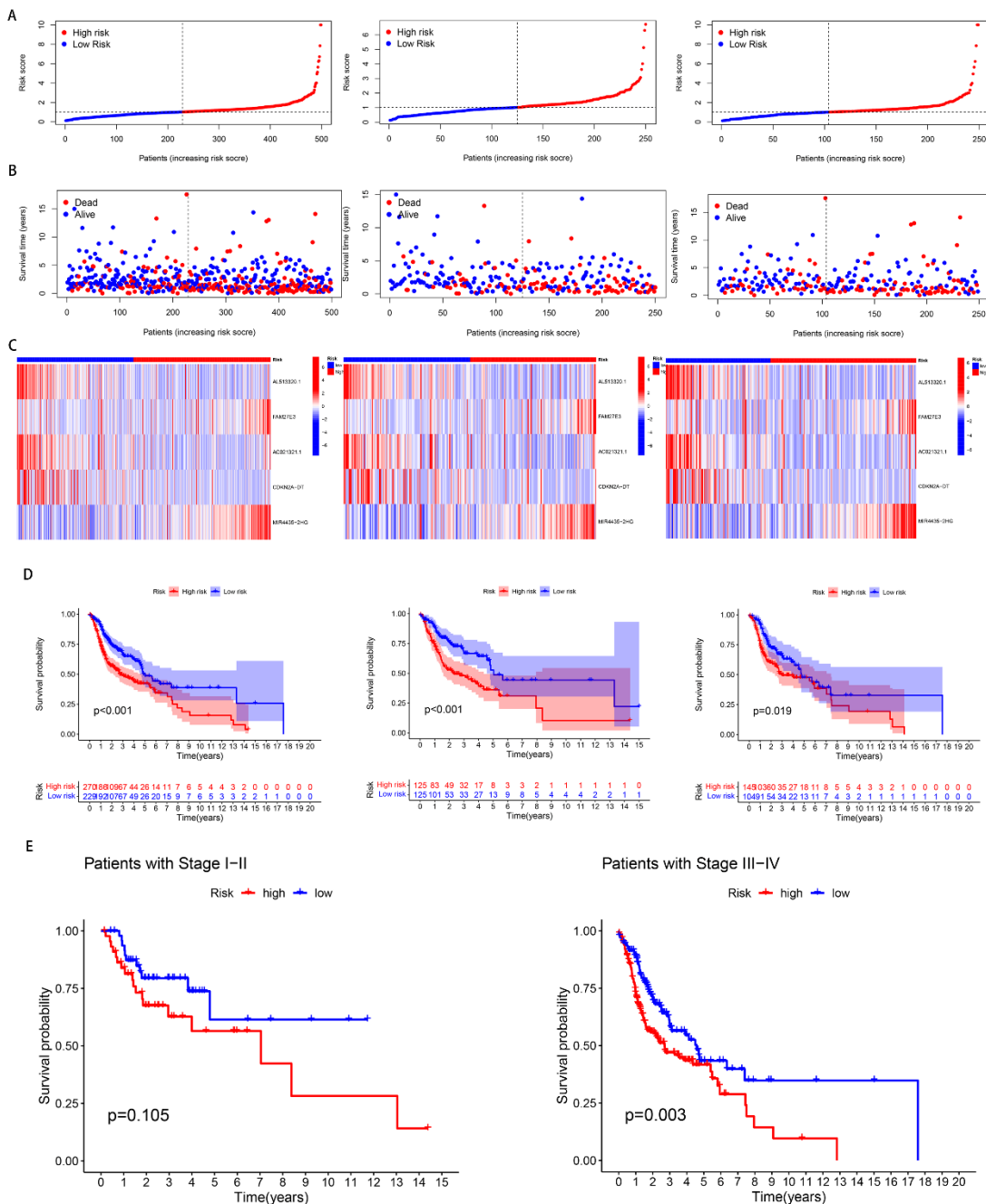


Figure 2. Screening and analysis of the value of cuproptosis-related lncRNAs associated with the prognosis of HNSCC. (A) Univariate regression analysis of 16 cases of cuproptosis-related lncRNAs associated with overall survival. (B) Heat map of the gene expression of 16 prognostic cuproptosis-related lncRNAs. (C) ten-fold cross-validation for variable selection in the LASSO model. (D) LASSO coefficient profile of 16 cuproptosis-related lncRNAs. (E) Sankey diagram of cuproptosis-related lncRNAs.



### 3.3 Line diagram construction and verification

The age, tumor stage, and RS were significant independent prognostic variables in both uni-Cox and multi-Cox regression (Figure 4A and 4B,  $p < .05$ ). Figure 4C shows the line chart created to forecast the 1-, 2-, and 3-year survival rates of patients with HNSCC and the calibration curve that was created.

### 3.4 Assessment of risk models

OS at 1, 2, and 3 years was the study outcome, with AUCs of 0.671, 0.618, and 0.559, respectively (Figure 4D). At the same time, the ROC curves of RS, age, sex, clinical grade and stage were also drawn. The results show that the AUCs were 0.671, 0.580, 0.500, 0.544 and 0.559, respectively, indicating good predictive ability (Figure 4E).

### 3.5 GSVA

Figure 4G shows the signaling pathways regulated by the differentially expressed RNAs in the high-risk group. Most of them were connected to tumor incidence and growth. Owing to its central location among other signaling pathways, the mitogen-activated protein kinase (MAPK) signaling pathway plays a significant role in numerous signaling pathways involved in cell proliferation. We previously found that p38 MAPK was crucial for controlling the motility, invasion, and transformation of cancer stem cells, which affect tumorigenesis<sup>9</sup>. In the development and prognosis of tumor cells, immune-associated signaling pathways, such as the JAK-STAT signaling system, are closely connected. For example, JAK-STAT signaling pathway and *STAT3* and *STAT5* genes are abnormally activated in HNSCC cells. Activation of the *STAT3* and *STAT5* signal transduction pathways increases the expressions of downstream target genes, thereby improving cell proliferation, survival, angiogenesis, and immune system evasion<sup>10</sup>.



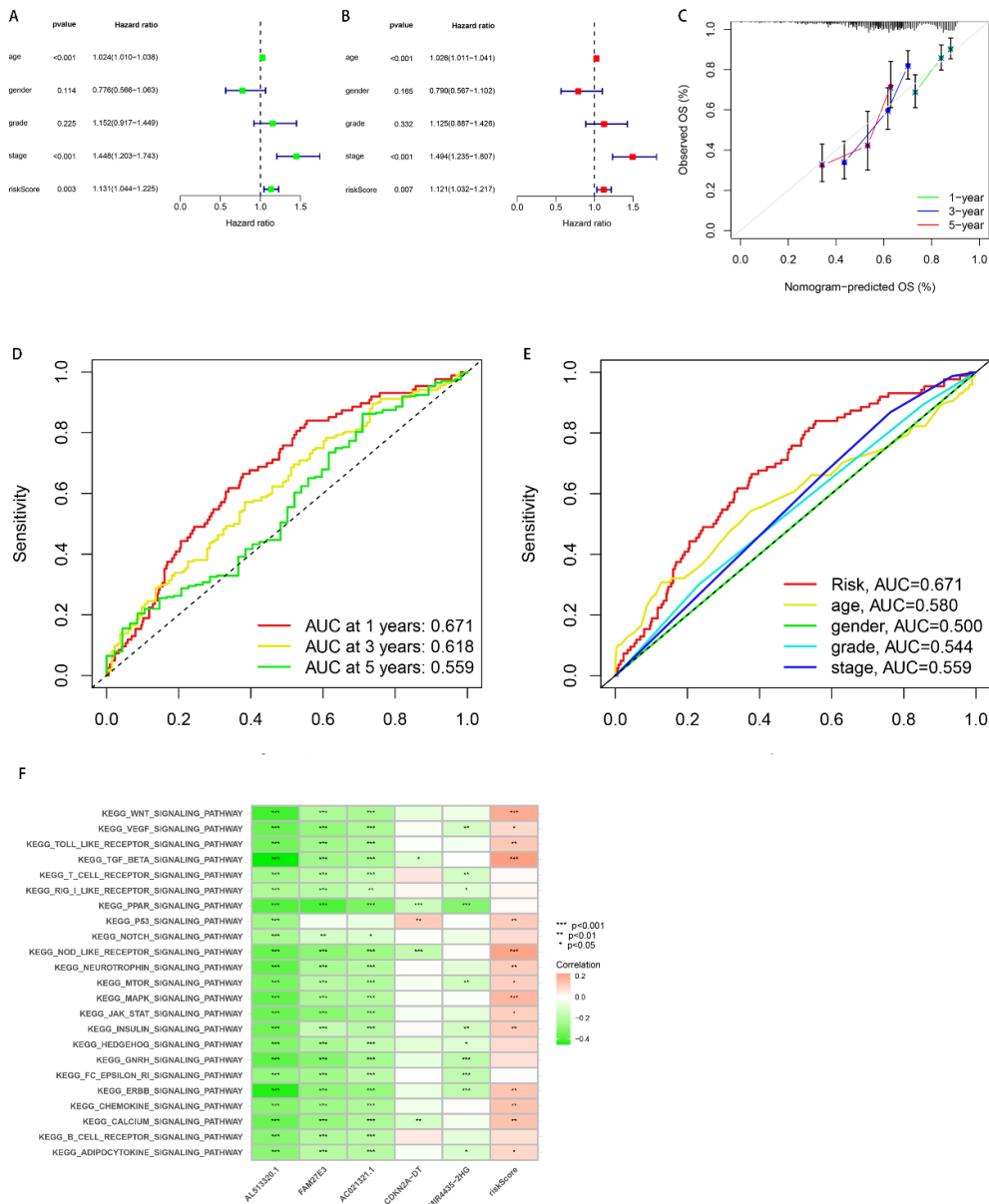


Figure 4. Nomogram and clinical factors of the risk model, AUC of the risk model. (A, B) univariate and multivariate Cox regression of clinical factors and RS with OS. (C) Nomogram with integrated RS, age, and tumor stage predicting the probability of the 1-, 2-, and 3-year OS. AUC of the risk model. (D) Calibration curves for 1-, 2-, and 3-year OS. (E) ROC curves for the 1-, 2-, and 3-year OS of the overall, training, and test sets. (F) GSVA of five prognostic cuproptosis-related lncRNAs in the high-risk group.

### 3.6 Investigation and clinical treatment of immune factors in the high-risk group

To explore the association between HNSCC and TME, the proportion of tumor-invasive immune cells in patients with HNSCC was calculated. The higher concentration of infiltrating immune cells was observed in the high-risk group, including activated myeloid dendritic cells, endothelial cells, mast cells, the immune score in xCell, T-cell CD4<sup>+</sup> memory resting, natural killer cells in EPIC, and M2 macrophages in CIBERSORT (Figure 5A). Cellular components in TME can define the immunophenotype of cancer and thus affect the patient prognosis<sup>11</sup>. In TME with higher RSs, many cytokines and immunosuppressive cells were linked to tumor immune evasion (Figure 5B). The high-risk group had higher ImmuneScore, StromalScore, and ESTIMATEScore (Figure 5C), indicating that TMEs differ between the high- and low-risk groups. Therefore, TME should be incorporated, and immunotherapy management should be optimized. Because immune checkpoint expression is important for immunotherapy, we investigated the relationships between high- and low-risk groups and immune checkpoint molecules. High- and low-risk groups showed discrepancies in immune checkpoint molecules (Figure 5D). This result could provide a reference for more suitable immune checkpoint inhibitors for patients according to RS during immunotherapy. Because immunotherapy drugs also cause adverse reactions, and the same patients can respond differently to the same drugs, we explored the relationship between RS and chemotherapy resistance. According to IC50 calculated by R package, the two groups differed in drug sensitivity. Patients in the low-risk group were significantly more responsive to AKT. Inhibitor.VIII, EHT.1864, and methotrexate, while those in the high-risk group were significantly more sensitive to gefitinib, dasatinib, and BMS.754807 (Figure 5E,  $p < .01$ ).

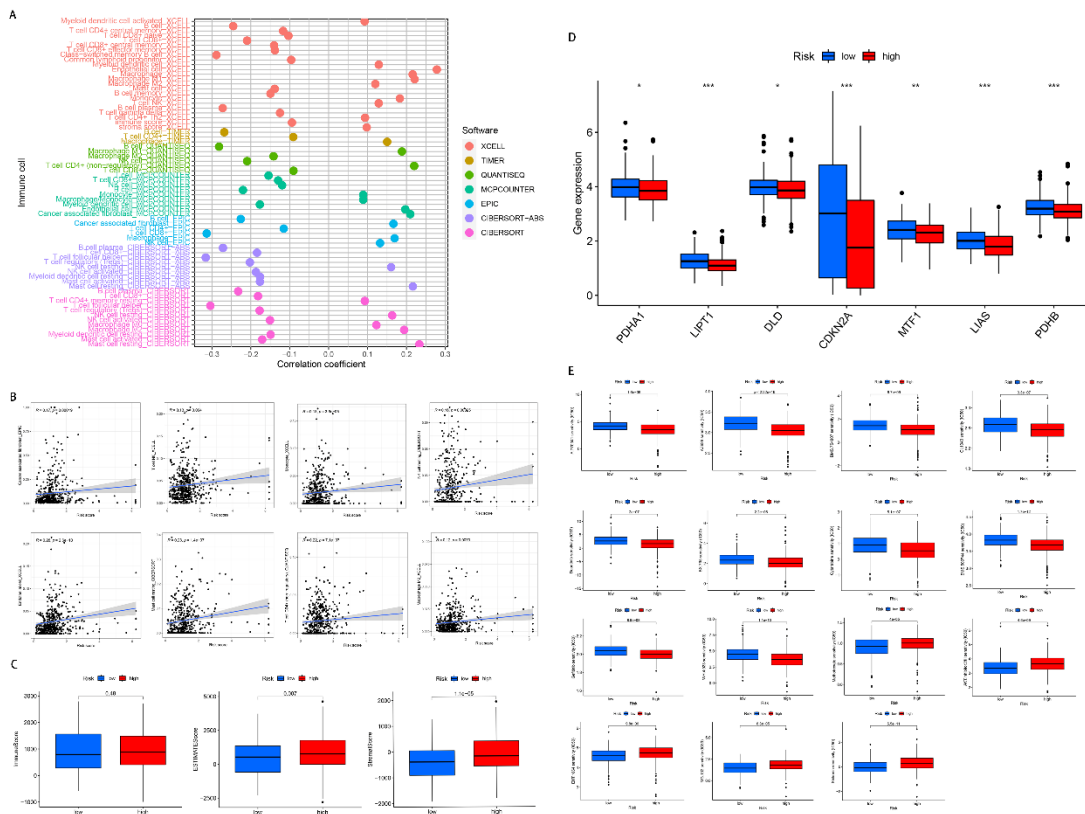
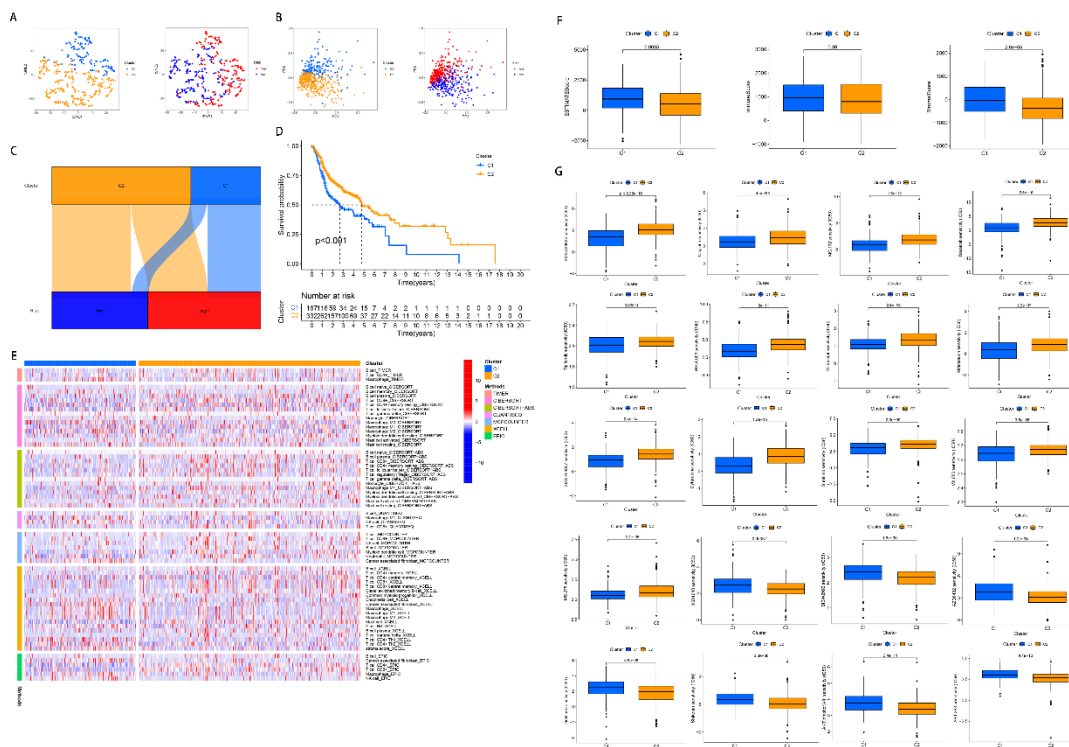


Figure 5. Cuproptosis-related lncRNAs and immunotherapy. (A) Immune cell bubble of risk groups on different platforms. (B) Correlation between RS and immune cells. (C) Comparison of immune-related scores between the low- and high-risk groups. (D) Difference in the expressions of seven checkpoints between the low- and high-risk groups. (E) IC50 for immunotherapy agents in the low- and high-risk groups.

### 3.7 Differentiation of hot and cold tumors and exploration of their roles

Tumors can be divided into subgroups with different immune microenvironments and different immunotherapeutic responses<sup>12,13</sup>. The ConsensusClusterPlus R software was used to cluster patients based on five cuproptosis-related lncRNAs. The two separated clusters were plainly visible in the t-SNE data (Figure 6A). PCA verified that risk groups and clusters correlated with each other (Figure 6B). Furthermore, the “ggalluvial” R package demonstrated a substantial relationship between cluster 1 and the high-risk group and cluster 2 and the low-risk group (Figure 6C). The Kaplan–Meier analysis showed variations in survival between the two groups, with lower OS in cluster 1 (Figure 6D). In addition, we performed the TME analysis for both groups. Compared to cluster 2 cluster 1 had more immune cell infiltration (Figure 6E) and higher immune and microenvironment scores (Figure 6F). Thus, cluster 1 was of hot tumors, whereas cluster 2 was of cold tumors. Cold and hot tumors have different immunotherapeutic responses because of different TMEs<sup>14</sup>. Hot tumors have more immune cell infiltration, making them more responsive to immunotherapy drugs. To test this conclusion, drug sensitivity was compared between the two groups. According to IC50, we found that cluster 1 was more sensitive to many immunotherapy agents (Figure 6G)<sup>15</sup>.

Figure 6(below). Differentiation and immunotherapy prediction of hot and cold tumors. (A) t-SNE of risk groups and clusters. (B) PCA of risk groups and clusters. (C) Sankey diagrams for risk groups and clusters. (D) Kaplan–Meier survival curves of OS (survival probability) in clusters. (E) Heat map of immune cells in clusters. (F) Comparison of immune-related scores between clusters 1 and 2. (G) Differences in IC50 among 20 immunotherapy drugs.



#### 4. Discussion

Complications of HNSCC treatment include postoperative functional disability and cosmetic defects, risk of relapse because of incomplete hand excision<sup>16</sup>, and pharyngeal dysfunction, ototoxicity, neurotoxicity, and nephrotoxicity caused by chemotherapy. Therefore, novel therapeutic approaches are needed to improve outcomes for HNSCC patients and reduce the likelihood of treatment-related complications. Immunotherapy is currently providing considerable therapeutic advantages to many patients with cancer. The average survival rates for relapsed/metastatic HNSCC in patients undergoing immunotherapy and cisplatin or carboplatin, 5-fluorouracil, and cetuximab treatment were 21.9 and 10.1 months, respectively<sup>17,18</sup>. However, immunotherapy has certain limitations. The efficacy of immune checkpoint inhibitors is limited to select patients. The anti-tumor spectrum is narrow. Further, adverse reactions can occur. These shortcomings limit the practical application of immunotherapy. Determination of accurate tumor markers and more targeted immunotherapy drugs is important.

In immunotherapy, immune checkpoint inhibitors can release existing immune response to kill tumors. Without existing immune response, the effective rate of immune checkpoint inhibitors ranges from 10% to 35%. Most stage IV solid tumors have no or few infiltrating T lymphocytes in the primary tumor at the time of diagnosis, which may explain the response rate to immune checkpoint inhibitors. These patients do not respond well to immune checkpoint inhibitors, leading to ineffective and poor efficacy of immunotherapy. Faced with immunotherapy's limitations owing to immune checkpoint inhibitors' low response rate in these patients and immunotherapy's poor efficacy, we introduced the concepts of cold and hot tumors in this context, providing novel ideas for immunotherapy. Cold tumors can transform into hot tumors, with experimentally verified feasibility<sup>8</sup>. In TCGA dataset and human tissue samples, macrophages in patients with HNSCC were significantly overexpressed in cancer tissues than in adjacent tissues<sup>19</sup>. By phenotype, macrophages are divided into M1 and M2 types. When a macrophage is polarized to the M2 type, it can promote tumor cell invasion, metastasis, and epithelial-to-mesenchymal transition (EMT), and by interfering with it, the migration of tumor cells has reduced speed and aggressiveness. The M2 macrophage can also promote tumor immune evasion and exhaust T cells through a high surface expression of the programmed cell death protein 1 (PD-1) receptors PD-L1 and PD-L2. In addition, hot tumors with more infiltrating immune cells show more effectiveness of immunotherapy<sup>20</sup>. We comprehensively analyzed lncRNA expression profiles of patients with HNSCC from TCGA database combined with cuproptosis-regulated genes and related the clinical information. Finally, five prognosis-related lncRNAs were extracted, and a prognostic risk model was established. Patients were divided into high- and low-risk groups according to RS, and accuracy and effectiveness in the high- and low-risk groups were verified. However, based only on RS, we are still unable to distinguish between cool and hot tumors. Reporter subtypes, or molecular subtypes, have been linked to tumor immunosuppression and TME<sup>21</sup>. Immune and TME scores are related to tumor subtypes, which in turn lead to different prognoses and immunotherapeutic responses<sup>14</sup>. The patients were divided into two groups based on the expression of cuproptosis-related lncRNAs in HNSCC<sup>22</sup>. The results of the analysis supported our hypothesis that the two clusters have different immune microenvironments. Cluster 1 had more immune cell infiltration, such as of macrophage M2, and a higher immune score. Further, the immunotherapy drugs were stronger. Therefore, cluster 1 could be considered to contain hot tumors.

*MTF1* expression in HNSCC may be associated with lymph node or distant metastasis, as shown by the Sankey diagram of *MIR4435-2HG* and *SLBP-DT*<sup>23</sup>. *MIR4435-2HG*, or *LINC00978* and *AK001796*, is upregulated in some cancers, such as



colorectal, bladder, breast, stomach, hepatocellular, lung, head and neck, etc.<sup>24-26</sup>. *MIR4435-2HG* overexpression in a study by Luo et al.<sup>27</sup> was linked to cisplatin resistance in colon cancer cells. HCT116. Cisplatin has clinical efficacy for various solid tumors, including HNSCC. *MIR4435-2HG* overexpression may cause failure to achieve good results in clinical treatment with cisplatin. Knocking-down the *MIR4435-2HG* expression in liver cancer cells significantly decreases the proliferation of liver cells. Knocking-down *MIR44353HG* expression inhibited bladder cancer cell proliferation and migration, whereas *MIR44353HG* overexpression promoted bladder cancer cell proliferation and migration<sup>28</sup>. In colorectal cancer, *MIR4435-2HG* participates in tumor cell proliferation and metastasis by regulating the miR-206/YAP1 axis and silencing *MIR4435-2HG* in cancer cells. The proliferative capacity of colorectal cancer cells was significantly downregulated<sup>29</sup>. *Kras* mutations occur in many tumor cells. They can lead to accelerated cell proliferation and maintain the strong proliferation ability of tumor cells. Excessive proliferation of tumor cells leads to hypoxia in the tumor. Over time, EMT occurs in tumor tissues. The synergistic effect of *Kras* and *YAP1* is mutually reinforcing<sup>30</sup>. In an in vitro study on HNSCC, *MIR44352HG* downregulation inhibited tumor cell proliferation, invasion, and EMT, and the mechanism may be related to the miR-383-5p/RBM3 axis. *MIR4435-2HG* has also been implicated in glycolysis and immune infiltration in cancer and been differentially expressed in tumors that are more amenable to immunotherapy<sup>31</sup>. *PDHA1* is associated with *FAM27E3*. Its downregulation is linked to a poor prognosis of various tumors, and its downregulation can lead to increased IC50<sup>32-35</sup>. *LIPT1* is connected to *AL513320.1*, a predictor of patient outcome in liver cancer. Its expression corresponds with patient survival in bladder cancer<sup>3</sup>. *FAM27E3*, *AC021321.1*, or *SLBP-DT* has not been studied. Studies on *AL513320.1* are also relatively few. In-depth research of the link between lncRNAs and tumors would provide insight into the clinical management.

Model construction could help screen high-risk patients, judge the survival prognosis, and provide novel directions for diagnostic models in clinical and scientific research. Early detection, diagnosis, and treatment of HNSCC help prolong survival. Therefore, a novel, efficient, and accurate diagnostic model should be established to diagnose and treat patients with hypertension. In this study, we used many methods to assess our model. The results were derived from multiple platforms. The prediction accuracy is high, which may be considered as external validation<sup>36</sup>.

## 5. Conclusion

Based on bioinformatics, we established a prognostic risk model to assess the outcomes of HNSCC and suggest relevant drugs to help clinicians formulate personalized treatment options. Cuproptosis-related lncRNAs could predict patient outcomes and help differentiate between hot and cold tumors, which might pave the way for novel therapeutic approaches that would significantly improve personalized treatment and outcomes.

## Conflicts of Interest

The authors declare that there are no conflicts of interest regarding the publication of this study.

## Data Availability

The data used to support the results are available at the TCGA (<https://www.cancer.gov/ccg/research/genome-sequencing/tcga>), GTEx (<https://www.genome.gov/Funded-Programs-Projects/Genotype-Tissue-Expression-Project>), GSEA (<https://www.gsea-msigdb.org/gsea/index.jsp>), and GDSC (<https://www.cancerrxgene.org/>).

## Acknowledgments A

This study was supported by the Talent Special Program of Youjiang Medical College for Nationalities Affiliated Hospital, China (YYFYR20213002) and the National Natural Science Foundation of China (81660495).

## References

1. Cohen EE, Bell RB, Bifulco CB, et al. The Society for Immunotherapy of Cancer consensus statement on immunotherapy for the treatment of squamous cell carcinoma of the head and neck (HNSCC). *Journal for immunotherapy of cancer*. 2019;7(1):1-31.
2. Yang F, Pei R, Zhang Z, et al. Copper induces oxidative stress and apoptosis through mitochondria-mediated pathway in chicken hepatocytes. *Toxicology In Vitro*. 2019;54:310-316.
3. Chen Y, Xu T, Xie F, et al. Evaluating the biological functions of the prognostic genes identified by the Pathology Atlas in bladder cancer. *Oncology Reports*. 2021;45(1):191-201.
4. Jiang N, Zhang X, Gu X, Li X, Shang L. Progress in understanding the role of lncRNA in programmed cell death. *Cell death discovery*. 2021;7(1):1-11.
5. Quinn JJ, Chang HY. Unique features of long non-coding RNA biogenesis and function. *Nature Reviews Genetics*. 2016;17(1):47-62.
6. Jiang S, Tan B, Zhang X. Identification of key lncRNAs in the carcinogenesis and progression of colon adenocarcinoma by co-expression network analysis. *Journal of Cellular Biochemistry*. 2019;120(4):6490-6501.
7. Dragomir MP, Kopetz S, Ajani JA, Calin GA. Non-coding RNAs in GI cancers: from cancer hallmarks to clinical utility. *Gut*. 2020;69(4):748-763.
8. Galon J, Bruni D. Approaches to treat immune hot, altered and cold tumours with combination immunotherapies. *Nature reviews Drug discovery*. 2019;18(3):197-218.
9. Wagner EF, Nebreda AR. Signal integration by JNK and p38 MAPK pathways in cancer development. *Nature Reviews Cancer*. 2009;9(8):537-549.

10. Geiger JL, Grandis JR, Bauman JE. The STAT3 pathway as a therapeutic target in head and neck cancer: Barriers and innovations. *Oral oncology*. 2016;56:84-92.
11. Wu J, Li L, Zhang H, et al. A risk model developed based on tumor microenvironment predicts overall survival and associates with tumor immunity of patients with lung adenocarcinoma. *Oncogene*. 2021;40(26):4413-4424.
12. Hardman C, Ho S, Shimizu A, et al. Synthesis and evaluation of designed PKC modulators for enhanced cancer immunotherapy. *Nature communications*. 2020;11(1):1-11.
13. Das S, Camphausen K, Shankavaram U. Cancer-specific immune prognostic signature in solid tumors and its relation to immune checkpoint therapies. *Cancers*. 2020;12(9):2476.
14. Zeng D, Li M, Zhou R, et al. Tumor Microenvironment Characterization in Gastric Cancer Identifies Prognostic and Immunotherapeutically Relevant Gene SignaturesCellular Landscape of Gastric Cancer TME and Relevant Signatures. *Cancer immunology research*. 2019;7(5):737-750.
15. Adib E, Nassar AH, Akl EW, et al. CDKN2A Alterations and Response to Immunotherapy in Solid TumorsCDKN2A Alterations and Response to Immunotherapy. *Clinical Cancer Research*. 2021;27(14):4025-4035.
16. Gavrieliatou N, Doumas S, Economopoulou P, Foukas PG, Psyrris A. Biomarkers for immunotherapy response in head and neck cancer. *Cancer treatment reviews*. 2020;84:101977.
17. Cramer JD, Burtneess B, Ferris RL. Immunotherapy for head and neck cancer: Recent advances and future directions. *Oral oncology*. 2019;99:104460.
18. Muzaffar J, Bari S, Kirtane K, Chung CH. Recent advances and future directions in clinical management of head and neck squamous cell carcinoma. *Cancers*. 2021;13(2):338.
19. Xue Y, Gao S, Gou J, et al. Platinum-based chemotherapy in combination with PD-1/PD-L1 inhibitors: preclinical and clinical studies and mechanism of action. *Expert opinion on drug delivery*. 2021;18(2):187-203.
20. Nikitina E, Larionova I, Choinzonov E, Kzhyshkowska J. Monocytes and macrophages as viral targets and reservoirs. *International journal of molecular sciences*. 2018;19(9):2821.
21. Ajani JA, Lee J, Sano T, Janjigian YY, Fan D, Song S. Gastric adenocarcinoma. *Nature reviews Disease primers*. 2017;3(1):1-19.
22. Wilkerson MD, Hayes DN. ConsensusClusterPlus: a class discovery tool with confidence assessments and item tracking. *Bioinformatics*. 2010;26(12):1572-1573.
23. Pavón MA, Parreño M, Téllez-Gabriel M, et al. CKMT1 and NCOA1 expression as a predictor of clinical outcome in patients with advanced-stage head and neck squamous cell carcinoma. *Head & neck*. 2016;38(S1):E1392-E1403.
24. Wang S, Chen X, Qiao T. Long non-coding RNA MIR4435-2HG promotes the progression of head and neck squamous cell carcinoma by regulating the miR-383-5p/RBM3 axis. *Oncology reports*. 2021;45(6):1-10.
25. Shen X, Ding Y, Lu F, Yuan H, Luan W. Long noncoding RNA MIR4435-2HG promotes hepatocellular carcinoma proliferation and metastasis through the miR-22-3p/YWHAZ axis. *American journal of translational research*. 2020;12(10):6381.
26. Fu M, Huang Z, Zang X, et al. Long noncoding RNA LINC 00978 promotes cancer growth and acts as a diagnostic biomarker in gastric cancer. *Cell proliferation*. 2018;51(1):e12425.
27. Luo P, Wu S, Ji K, et al. LncRNA MIR4435-2HG mediates cisplatin resistance in HCT116 cells by regulating Nrf2 and HO-1. *PLoS One*. 2020;15(11):e0223035.
28. Wang W, Xu Z, Wang J, Chen R. LINC00978 promotes bladder cancer cell proliferation, migration and invasion by sponging miR-4288. *Molecular Medicine Reports*. 2019;20(2):1866-1872.
29. Dong X, Yang Z, Yang H, Li D, Qiu X. Long non-coding RNA MIR4435-2HG promotes colorectal cancer proliferation and metastasis through miR-206/YAP1 axis. *Frontiers in oncology*. 2020;10:160.
30. Shen M, Zhou G, Zhang Z. LncRNA MIR4435-2HG contributes into colorectal cancer development and predicts poor prognosis. *European Review for Medical and Pharmacological Sciences*. 2020;24(4):1771-1777.
31. Ho K-H, Huang T-W, Shih C-M, et al. Glycolysis-associated lncRNAs identify a subgroup of cancer patients with poor prognoses and a high-infiltration immune microenvironment. *BMC medicine*. 2021;19(1):1-17.
32. Chen T-Y, Hsieh Y-T, Huang J-M, et al. Determination of pyruvate metabolic fates modulates head and neck tumorigenesis. *Neoplasia*. 2019;21(7):641-652.
33. Song L, Liu D, Zhang X, et al. Low expression of PDHA1 predicts poor prognosis in gastric cancer. *Pathology-Research and Practice*. 2019;215(3):478-482.
34. Liu L, Cao J, Zhao J, Li X, Suo Z, Li H. PDHA1 gene knockout in human esophageal squamous cancer cells resulted in greater Warburg effect and aggressive features in vitro and in vivo. *OncoTargets and therapy*. 2019;12:9899.
35. Zhuang L, Zhang B, Liu X, et al. Exosomal miR-21-5p derived from cisplatin-resistant SKOV3 ovarian cancer cells promotes glycolysis and inhibits chemosensitivity of its progenitor SKOV3 cells by targeting PDHA1. *Cell Biology International*. 2021;45(10):2140-2149.
36. Xu F, Huang X, Li Y, Chen Y, Lin L. m6A-related lncRNAs are potential biomarkers for predicting prognoses and immune responses in patients with LUAD. *Molecular Therapy-Nucleic Acids*. 2021;24:780-791.